

# Photochemistry of the $\pi$ -Extended 9,10-Bis(1,3-dithiol-2-ylidene)-9,10-dihydroanthracene System: Generation and Characterisation of the Radical Cation, Dication, and Derived Products\*\*

Allison E. Jones,<sup>[a]</sup> Christian A. Christensen,<sup>[a]</sup> Dmitrii F. Perepichka,<sup>[a]</sup> Andrei S. Batsanov,<sup>[a]</sup> Andrew Beeby,<sup>\*,[a]</sup> Paul J. Low,<sup>\*,[a]</sup> Martin R. Bryce,<sup>\*,[a]</sup> and Anthony W. Parker<sup>[b]</sup>

**Abstract:** Flash photolysis of bis[4,5-di(methylsulfanyl)1,3-dithiol-2-ylidene]-9,10-dihydroanthracene (**1**) in chloroform leads to formation of the transient radical cation species **1**<sup>•+</sup> which has a diagnostic broad absorption band at  $\lambda_{\text{max}} \approx 650$  nm. This band decays to half its original intensity over a period of about 80  $\mu\text{s}$ . Species **1**<sup>•+</sup> has also been characterised by resonance Raman spectroscopy. In degassed solution **1**<sup>•+</sup> dis-

proportionates to give the dication **1**<sup>2+</sup>, whereas in aerated solutions the photodegradation product is the 10-[4,5-di(methylsulfanyl)1,3-dithiol-2-ylidene]anthracene-9(10*H*)one (**2**). The dication **1**<sup>2+</sup> has been characterised by a spec-

troelectrochemical study [ $\lambda_{\text{max}}$  ( $\text{CH}_2\text{Cl}_2$ ) = 377, 392, 419, 479 nm] and by an X-ray crystal structure of the salt **1**<sup>2+</sup>( $\text{ClO}_4^-$ )<sub>2</sub>, which was obtained by electrocrystallisation. The planar anthracene and 1,3-dithiolium rings in the dication form a dihedral angle of 77.2°; this conformation is strikingly different from the saddle-shaped structure of neutral **1** reported previously.

**Keywords:** dithioles • electrochemistry • photolysis • radical ions • structure elucidation

## Introduction

Tetrathiafulvalene (TTF) is a famous  $\pi$ -electron donor molecule which undergoes two reversible one-electron waves to afford the radical cation and dication species,<sup>[1]</sup> with a gain in heteroaromaticity upon formation of the 1,3-dithiolium cation.<sup>[2]</sup> Considerable attention has been directed to related bis(1,3-dithiole) systems where  $\pi$ -conjugation is extended between the dithiole rings by the insertion of vinylogous<sup>[3]</sup> and quinonoid<sup>[4]</sup> spacer units; this leads to reduced intramolecular Coulombic repulsion in the oxidised states.<sup>[5]</sup> Derivatives of the 9,10-bis(1,3-dithiol-2-ylidene)-9,10-dihydroanthracene

system are particularly interesting in this context as they have a single, quasi-reversible, two-electron oxidation wave that yields a thermodynamically stable dication, for example, for **1**,<sup>[6]</sup>  $E^{\text{ox}} = +0.55$  V (in MeCN vs. Ag/AgCl) in the cyclic voltammogram.<sup>[7]</sup> The X-ray crystal structure of **1**<sup>[6]</sup> and several derivatives<sup>[8]</sup> have shown that a remarkable conformational change accompanies oxidation to the dication. Whereas the neutral molecules are saddle-shaped,<sup>[6, 8]</sup> with the central ring of the anthracenediylidene moiety in a boat conformation, the dications have a planar anthracene system with the 1,3-dithiolium cations almost orthogonal to this plane.<sup>[7b, 9]</sup> Theoretical calculations support the crystallographic data: steric hindrance between the sulfur atoms and the peri hydrogen atoms dictates the conformation of the neutral species whilst, in the dication, there is aromatisation of both the dithiolium rings and the anthracene core.<sup>[10]</sup> Calculations also suggest that the radical cation largely retains the saddle conformation of the neutral species, thereby restricting any potential gain in aromaticity at this redox stage; this is in accord with the electrochemical data.<sup>[10]</sup> The strong electron-donor ability of the title ring system has led to its use as a component of intermolecular<sup>[7b, 9]</sup> and intramolecular<sup>[11]</sup> charge-transfer systems.

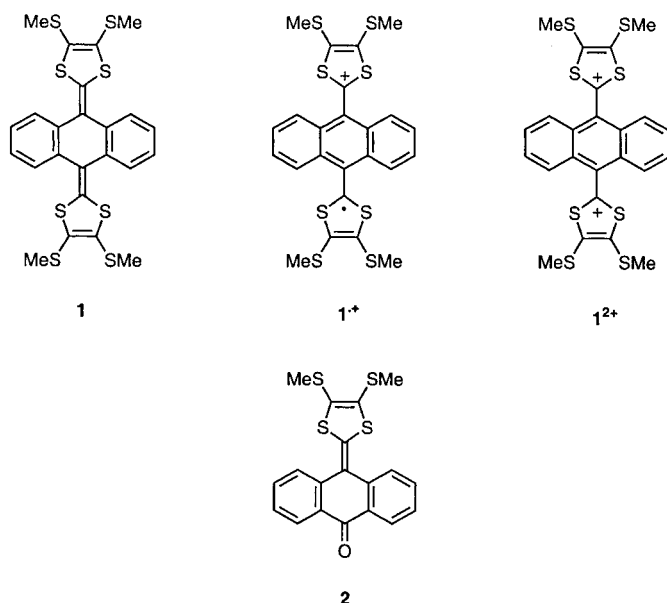
The aim of the present work was to explore the photolytic generation of the elusive  $\pi$ -radical cation species **1**<sup>•+</sup>. Herein we report the characterisation of **1**<sup>•+</sup> by UV/Vis and Raman

[a] Dr. A. Beeby, Dr. P. J. Low, Professor M. R. Bryce, A. E. Jones, C. A. Christensen, Dr. D. F. Perepichka, Dr. A. S. Batsanov  
Department of Chemistry, University of Durham  
Durham, DH1 3LE (UK)  
Fax: (+44) 191-384-4737  
E-mail: m.r.bryce@durham.ac.uk

[b] Dr. A. W. Parker  
Central Laser Facility, CLRC Rutherford Appleton Laboratory  
Chilton, Didcot, Oxfordshire, OX11 0QX (UK)

[\*\*] Molecular Saddles, Part 6; for Part 5 see ref. [8b].

Supporting information for this article is available on the WWW under <http://www.wiley-vch.de/home/chemistry/> or from the author: fluorescence spectra obtained by pump (266 nm)–probe (514 nm) of **1** in degassed chloroform.



spectroscopy, and we identify its decomposition products, namely, the dication **1<sup>2+</sup>** and the ketone **2**. The spectroelectrochemistry of **1** and the X-ray crystal structure of the electrocrystallised salt **1<sup>2+</sup>**(ClO<sub>4</sub><sup>-</sup>)<sub>2</sub> obtained during the course of this study are also discussed. While our work was in progress, Guldi et al. reported that **1<sup>•+</sup>** can be generated by pulse radiolysis of **1** in oxygenated CH<sub>2</sub>Cl<sub>2</sub> solution. Species **1<sup>•+</sup>**, generated in this way, was characterised by an absorption at  $\lambda_{\text{max}} = 675 \text{ nm}$ <sup>[11d, 12]</sup> and was stable over several hundred  $\mu\text{s}$  with no significant decay on the pulse radiolytic timescale (i.e., 1 ms).<sup>[12]</sup>

## Results and Discussion

**Spectroelectrochemistry of compound 1:** In order to obtain a reference spectrum of the dication **1<sup>2+</sup>**, a UV/Vis spectroelectrochemical study was undertaken. Previous electrochemical studies<sup>[7]</sup> have demonstrated that derivatives of **1** undergo a two-electron oxidation to yield the corresponding dication **1<sup>2+</sup>**. Electrolysis of **1** in dichloromethane was performed in an optically transparent thin-layer electrode (OTTLE) cell. Complete electrolysis of the sample within the thin-layer region was achieved, as indicated by the vanishingly small currents which flowed through the cell and the observation of identical absorption profiles at applied potentials of 0.65, 0.75 and 0.85 V. Reduction in situ, which led to the recovery of the initial spectrum, confirmed the full reversibility of the redox system under these conditions. The compiled spectra (Figure 1) also contain clean isobestic points marking the conversion of the neutral to the dicationic species.

The spectrum of the neutral species **1** consists of two strong bands at  $\lambda_{\text{max}} = 366$  and 435 nm. During electrolysis these collapse giving way to bands ascribed to the species **1<sup>2+</sup>** at  $\lambda_{\text{max}} = 377$ , 392 and 419 nm, and a broad band which tails into the visible portion of the spectrum with  $\lambda_{\text{max}} = 479 \text{ nm}$ .

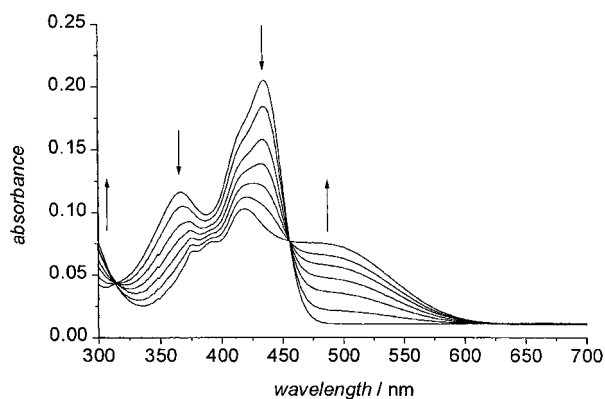


Figure 1. Spectroelectrochemistry of compound **1** in dichloromethane. (For conditions see the Experimental Section).

Neither neutral **1** nor the electrolytically generated dication gives rise to any significant absorption between 650–1000 nm. The spectrum of **1<sup>2+</sup>** obtained by this in situ electrochemical method was identical to that obtained by the dissolution in acetonitrile of an authentic sample of **1<sup>2+</sup>**(ClO<sub>4</sub><sup>-</sup>)<sub>2</sub> (obtained by electrocrystallisation, see below).

**Steady state photolysis of compound 1:** Irradiation of **1** in aerated chloroform by using the output of a Xe lamp ( $\lambda_{\text{ex}} = 320\text{--}600 \text{ nm}$ ) brought about a marked change in the UV/Vis absorption spectrum of the solution, as illustrated in Figure 2.

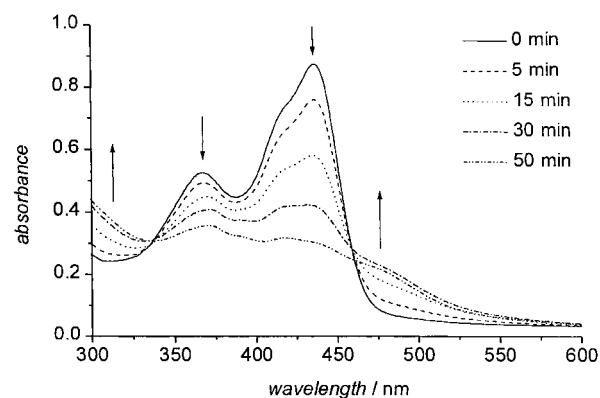


Figure 2. UV/Vis spectrum of **1** in aerated chloroform, irradiated by the filtered output of a Xe lamp (320–650 nm).

The photoproduct from this reaction was isolated and its UV/Vis and fluorescence spectra are shown in Figure 3. This product is unambiguously identified as the ketone **2** on the basis that its melting point, TLC behaviour, mass spectrum and <sup>1</sup>H NMR and UV/Vis spectra were identical with an authentic sample synthesised from anthrone.<sup>[6]</sup> Significantly, the UV/Vis spectrum of **2** is markedly different from that of the dication **1<sup>2+</sup>**. Irradiation of **1** in degassed chloroform resulted in a change in the UV/Vis spectrum, consistent with the formation of the dication **1<sup>2+</sup>** (Figure 4). There was no evidence for the formation of ketone **2** under these conditions.

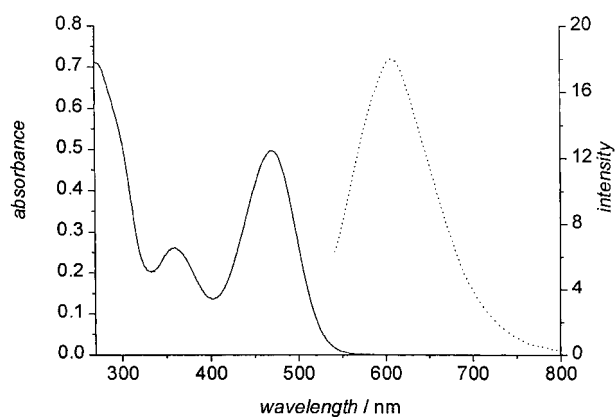


Figure 3. UV/Vis absorption (left) and corrected fluorescence emission spectrum (right) of **2** in chloroform solution. An excitation wavelength of 460 nm was used for recording the emission spectrum.

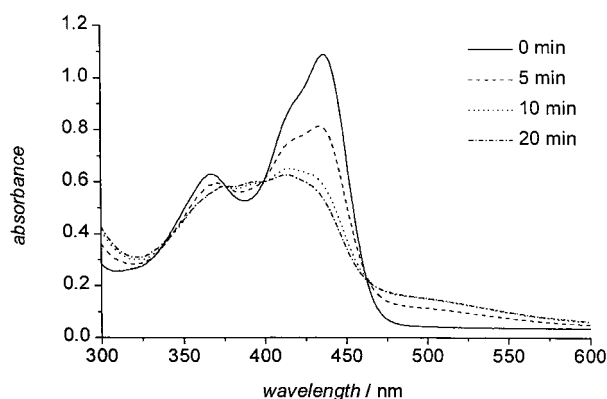


Figure 4. UV/Vis spectrum of **1** in degassed chloroform, irradiated by the filtered output of a Xe lamp (320–600 nm).

In an attempt to elucidate the mechanism of the formation of **2**, we investigated the role of singlet oxygen. Time-resolved near-IR luminescence experiments<sup>[13]</sup> showed no evidence for the production of singlet oxygen,  $\phi_{\Delta} < 0.001$ , by **1**, **2** or  $\mathbf{1}^{2+}(\text{ClO}_4^-)_2$  in acetonitrile. However, we did observe that in toluene solution, **1** rapidly quenches the singlet oxygen produced by an added photosensitiser (zinc tetraphenylporphyrin) and rapidly degrades to form **2** with a rate constant of  $2.9 \pm 0.1 \times 10^7 \text{ mol}^{-1} \text{ dm}^3 \text{ s}^{-1}$ .

**Time-resolved studies:** Flash photolysis of **1** in degassed chloroform revealed a transient species with an absorption band at  $\lambda_{\text{max}} \approx 650 \text{ nm}$  upon excitation at 355, 308 or 266 nm (Figure 5). This spectrum is consistent with that obtained by Guldi et al. for  $\mathbf{1}^{+}$  generated by pulse radiolysis of **1** in oxygenated dichloromethane.<sup>[12]</sup> This transient absorption decays as a nonexponential function (Figure 6); the signal-to-noise ratio obtained during the course of the experiments did not allow us to differentiate between a double exponential and a second-order decay. Under the conditions used, the transient absorption decayed to half its initial intensity over a period of about 80  $\mu\text{s}$  and the decay was not significantly affected by aeration of the solution. This indicates that the transient species is unlikely to be an excited (triplet) electronic state of the parent **1**. The same species was also

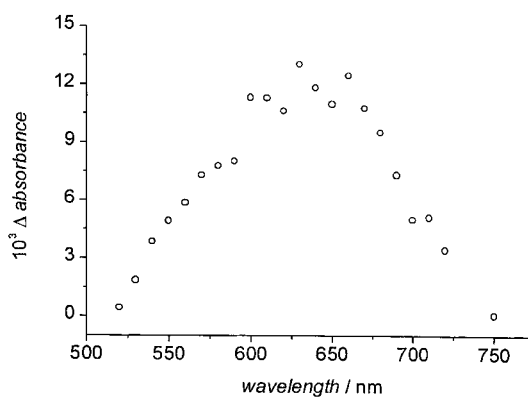


Figure 5. Transient absorption spectrum obtained upon 266 nm irradiation of **1** in degassed chloroform.

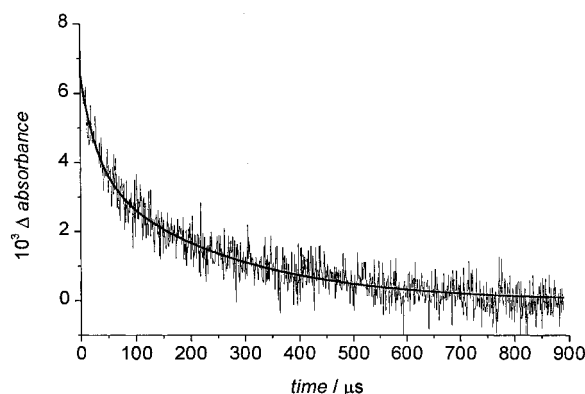


Figure 6. Transient absorption band at 630 nm produced upon irradiation of a degassed solution of **1** in chloroform. The decay is nonexponential and has a trend line added as a guide:  $\lambda_{\text{probe}} = 630 \text{ nm}$ .

observed in dichloromethane, but could not be observed when propionitrile or tetrahydrofuran was used as solvent. Based on our observations, we propose that the transient absorption arises from the radical cation  $\mathbf{1}^{+}$ , formed by a monophotonic photoionisation of the neutral **1**. The halogenated solvents play an important role by acting as a sink for the ejected photoelectrons according to the mechanism in Equation (1):



In aerated solutions, the halomethyl radicals may further oxidise to form  $\text{CH}_n\text{Cl}_{3-n}\text{O}_2 \cdot$ . However, the suggestion that this peroxyhalomethyl radical can oxidise **1** to  $\mathbf{1}^{+}$ , as suggested by Guldi et al,<sup>[12]</sup> is in doubt, since we observe no evidence for the enhancement of the transient bands in aerated solutions. We suggest that ketone **2** is most likely formed by reaction of  $\mathbf{1}^{2+}$  with either a peroxyhalomethyl radical or molecular oxygen. Attempts to determine the quantum yield of radical ion formation were prevented due to the photodecomposition of the samples during the course of the measurements.

**Raman spectroscopy:** The Raman spectrum of compound **1** (Figure 7) is dominated by three intense bands at 1500, 1525 and 1575  $\text{cm}^{-1}$ ; this profile has similarities to the nonresonant Raman spectrum of anthracene.<sup>[14]</sup> These bands were assigned to phenyl C=C stretching modes. Photolytic formation of the

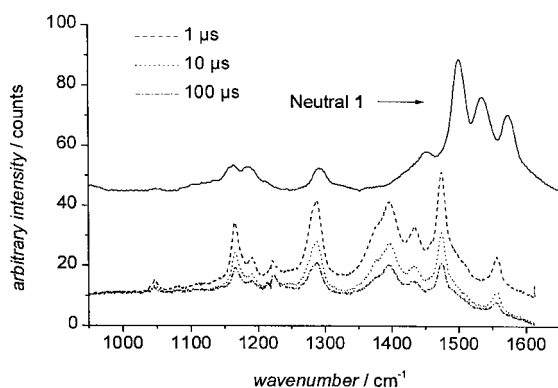


Figure 7. Ground state Raman spectrum of **1** recorded at 630 nm, and time resolved resonance Raman spectrum of  $\mathbf{1}^+$  recorded by using 266 nm pump and 630 nm probe: time delays are indicated. The spectra of  $\mathbf{1}^+$  are corrected by subtracting ground state and solvent bands (probe only).

radical cation  $\mathbf{1}^+$ , changes the spectral profile and yields a much richer array of bands. The highest resonant Raman band is observed at  $1560\text{ cm}^{-1}$ . This wave number value is less than for a typical aromatic C=C stretch and reflects a lowering of the aromatic C=C bond order following the loss of an electron from a bonding MO. Key points of interest are whether the anthracene moiety of  $\mathbf{1}^+$  retains the folded conformation of the neutral species<sup>[6]</sup> or is planar, and whether there is a “pseudo-quinoid” type structure, with the carbon–carbon bonds exocyclic to C9 and C10 displaying partial double bond character. In a recent investigation of the radical cation of an ethylene-bridged thiophene-based oligomer, an intense band was observed at  $1411\text{ cm}^{-1}$ ; in the neutral oligomer this is observed at about  $1430\text{ cm}^{-1}$ . These values (in the range  $1340$  to  $1430\text{ cm}^{-1}$ ) are typical for C=C modes in thio ring (e.g. thiophene) systems and it is likely that the broad feature at  $1390$  in  $\mathbf{1}^+$  resembles such a stretch.<sup>[15]</sup> In resonance Raman spectra, however, specific enhancement (Franck–Condon, A-term resonance enhancement) occurs for modes associated with the particular chromophore responsible for the electronic absorption at the laser wavelength chosen. The richness of the spectrum, as well as the intensity of the bands, probably indicates a very delocalised chromophore system that supports a “quinoid”-type framework. We note that theoretical calculations by Ortí et al. also suggest that the radical cation largely retains the saddle conformation of the neutral species.<sup>[10]</sup> Future investigations will be directed towards establishing this.

Attempts to probe the formation of  $\mathbf{1}^{2+}$  by using a pump/probe combination of 266/514 nm, respectively, failed to yield Raman spectra, due to fluorescence from the samples. However, it was found that the intensity of the fluorescence signal increased with the delay time between the pump and probe pulses. Furthermore, the spectral profile of this fluorescence ( $\lambda_{\text{max}} = 680\text{ nm}$ ) was clearly characteristic of the dication  $\mathbf{1}^{2+}$ , as shown by comparison with an in situ electrochemically generated sample. The fluorescence from ketone **2** is much more intense and emits at a shorter wavelength ( $\lambda_{\text{max}} = 630\text{ nm}$ ). This observation is consistent with the disproportionation of the radical cation according to Equation (2):



Thus, the nonfluorescent radical cation, which is formed immediately upon irradiation by the 266 nm pump pulse, forms the fluorescent dication  $\mathbf{1}^{2+}$  in *degassed* solution, this process occurring over a period of tens of microseconds. In contrast, in *aerated* solution, ketone **2** is the major product, with only traces of  $\mathbf{1}^{2+}$  detected.

**X-ray crystal structure of  $\mathbf{1}^{2+}(\text{ClO}_4^-)_2$ :** To establish the structure of the electrochemically generated product beyond doubt, X-ray structural analysis was performed on crystals that grew on the anode during the electrolysis of **1** in dichloromethane in the presence of tetrabutylammonium perchlorate. The X-ray data confirmed that **1** is oxidised to the dication under these conditions. In the crystal structure of  $\mathbf{1}^{2+}(\text{ClO}_4^-)_2$ , the anion occupies a general position, while the dication has crystallographic  $C_i$  symmetry (Figure 8). The

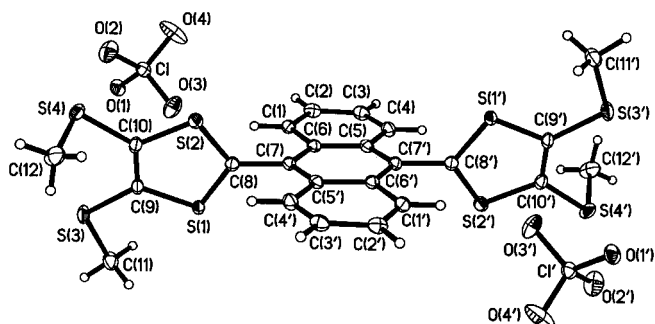


Figure 8. Molecular structure of  $\mathbf{1}^+(\text{ClO}_4^-)_2$  showing 50% thermal ellipsoids. Primed atoms are generated by the inversion centre.

anthracene moiety is planar and has essentially the geometry of the anthracene molecule,<sup>[16]</sup> that is, it is fully aromatic. The 1,3-dithiolium rings are also planar and display stronger  $\pi$ -conjugation than in the neutral molecule **1**. The C–S bonds in the dication (“inner” S1–C8  $1.695(2)$  and S2–C8  $1.672(2)$  Å; “outer” S1–C9  $1.734(2)$  and S2–C10  $1.708(2)$  Å) are contracted compared with neutral **1**<sup>[6]</sup> with averages  $1.767(4)$  and  $1.759(5)$  Å for the “inner” and “outer” C–S bonds, respectively, while the C9–C10 bond is lengthened from  $1.334(7)$  Å in **1** to  $1.375(3)$  Å in  $\mathbf{1}^{2+}(\text{ClO}_4^-)_2$ . The anthracene and dithiolium systems form a dihedral angle of  $77.2^\circ$  and are linked through an essentially single bond: C7–C8  $1.490(3)$  Å. The methylsulfanyl substituents have different conformations: the S3–C11 bond is coplanar with the dithiolium ring, while the S4–C12 bond makes an angle of  $80^\circ$  with this plane. The in-plane group is conjugated with the ring, as shown by the difference in the bond lengths C9–S3  $1.732(2)$  and C10–S4  $1.760(2)$  Å. The crystal packing of  $\mathbf{1}^{2+}(\text{ClO}_4^-)_2$  is shown in Figure 9. Interactions of the S1 atom with two perchlorate anions can explain the weakening of the S1–C bonds in the dithiolium ring compared with the S2–C bonds. There are no S...S contacts significantly shorter than twice the van der Waals radius of S ( $3.68\text{ Å}$ ).<sup>[17]</sup>

## Conclusion

The work described above has provided conclusive evidence for the existence of the elusive, transient radical cation  $\mathbf{1}^+$  formed by photoionisation of the neutral system **1** in

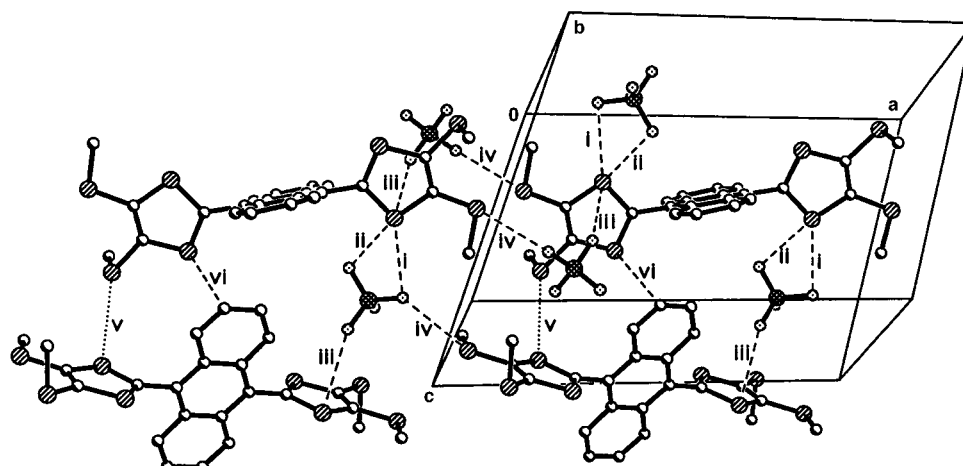


Figure 9. Crystal packing of  $1^{2+}(\text{ClO}_4^-)_2$ . Shortest intermolecular contacts (in Å): S...O i = 3.335(2), ii = 3.205(2), iii = 3.277(2), iv = 3.157(2); S...S v = 3.655(1); S...C vi = 3.450(2).

chlorinated hydrocarbon solutions. This radical cation has been characterised by transient absorption and resonance Raman spectroscopy. In degassed solution, this species appears to disproportionate to give the dication  $1^{2+}$ , which has been characterised by spectroelectrochemical techniques; its X-ray crystal structure has also been determined. Photolysis of aerated solutions of **1** also lead to formation of the radical cation, but the photodegradation product observed in these solutions is ketone **2**. The mechanism of the formation of **2** remains uncertain. Only traces of the dication  $1^{2+}$  are detected in aerated solutions.

## Experimental Section

**General details:** Spectroelectrochemical data were recorded for compound **1** (0.35 mM) in  $\text{CH}_2\text{Cl}_2$  with  $\text{NBu}_4\text{PF}_6$  (0.1 M) as supporting electrolyte, a Pt gauze working electrode and Pt wire counter and reference electrodes, on a Varian Cary 5 spectrophotometer between 300–1000 nm at ambient temperature. Spectra were corrected for background absorption arising from the cell, the electrolyte and the working electrode. The OTTL cell used a Pt gauze working electrode, Pt wire counter electrode and pseudo reference electrodes. The solutions were analysed in situ. The working electrode was held at a potential at which no electrochemical work was being done in the cell and the spectrum of neutral **1** was recorded. The potential was then increased in 50–100 mV increments and held until equilibrium had been obtained, as evidenced by a sharp drop in cell current. The cell was based upon that described elsewhere,<sup>[18]</sup> and was driven by a home-built potentiostat. For time-resolved resonance Raman spectroscopy the pump laser pulse (266 nm, 5 ns pulse width) was produced from the quadrupled output of a Spectra-Physics GCR-11. The probe pulse was generated from a Lumonics Pulsemaster PM-800 excimer (XeCl, 308 nm, 15 ns pulse width) pumping a Lambda-Physik FL3002 dye laser by using Rhodamine 101 dye to produce 630 nm light. Synchronisation of the two lasers was better than  $\pm 5$  ns. Pulse energies at the sample were about 0.5 to 1 mJ per pulse for both lasers which ran at 10 Hz. Raman spectra were obtained by using a  $90^\circ$  collection geometry with the liquid sample passed through a capillary (2 mm internal diameter) held perpendicular to the spectrograph collection optics and entrance slit. For in situ electrochemical generation, a Pt gauze working electrode and Pt wire counter- and pseudo-reference electrodes were inserted at each end of the capillary. The spectrograph was an Acton Research Corporation Spectra-Pro 500. Rayleigh scattered light was prevented from entering the spectrograph by using a holographic notch filter (Kaiser). Light was detected by a thinned, back-illuminated liquid nitrogen charge-coupled device camera (Princeton Instruments LN/CCD-1024 TKB) which was controlled by a PC and the

manufacturer's supplied software. Typical accumulation times were 200 s. Raman spectra were accurate to  $5\text{ cm}^{-1}$  and were calibrated by using literature values for toluene.<sup>[14]</sup>

**Preparation of  $1^{2+}(\text{ClO}_4^-)_2$ :** Dry tetrabutylammonium perchlorate (50 mg) was added to each chamber of a glass electrocrystallisation cell, in which the two chambers were separated by a glass frit, and the cell was flushed with argon. A solution of compound **1**<sup>[6]</sup> (5 mg) in dry degassed dichloromethane (7 mL) was placed in the anodic chamber. Dry degassed dichloromethane (7 mL) was placed in the cathodic chamber. The platinum electrodes were mounted, sealing the solutions from the atmosphere. A potential of 1.0 V was applied, which provided an initial current of  $2.0\ \mu\text{A}$ . The cell was stored in the dark for 2 days at  $20^\circ\text{C}$ , during which time the current dropped to  $0.5\ \mu\text{A}$  and red blade-shaped crystals of  $1^{2+}(\text{ClO}_4^-)_2$  up to 5 mm in length grew on the anode. The crystals were harvested and washed with dry dichloromethane.  $^1\text{H NMR}$  ( $(\text{CD}_3)_2\text{SO}$ ):  $\delta$  = 8.12 (m, 4H), 7.81 (m, 4H), 3.00 (s, 12H).

**Photolysis of **1**.** A solution of **1** in degassed chloroform sparged with nitrogen was irradiated for 1 h by the output of a Xe lamp, which had been filtered through aqueous copper sulfate solution ( $\lambda_{\text{ex}}$  = 320–600 nm). The solution was then stored at  $0^\circ\text{C}$  for 7 days. Red needles of the salt  $1^{2+}(\text{X}^{2-})_n$  (probably X = Cl) were collected by filtration and washed with chloroform. The UV/Vis and  $^1\text{H NMR}$  spectra of this product were identical with those of electrocrystallised  $1^{2+}(\text{ClO}_4^-)_2$ .

A solution of **1**, irradiated in aerated chloroform under the same conditions as those described above, was evaporated in vacuo and chromatographed on a silica gel column by eluting with chloroform. The first yellow fraction consisted of unreacted compound **1**; this was followed by a red fraction which yielded compound **2** on evaporation. The TLC, m.p., MS, UV/Vis and  $^1\text{H NMR}$  spectra were identical with those of authentic **2**.<sup>[6]</sup>

**X-ray crystallography:** The X-ray diffraction experiment was carried out on a SMART 3-circle diffractometer with a 1 K CCD area detector by using graphite-monochromated  $\text{MoK}_\alpha$  radiation ( $\lambda = 0.71073\ \text{\AA}$ ) and a Cryostream (Oxford Cryosystems) open-flow  $\text{N}_2$  gas cryostat. The full sphere of the reciprocal space was covered by a combination of five sets of  $\omega$  scans; each set at different  $\varphi$  and/or  $2\theta$  angles. Reflection intensities were integrated by using the SAINT program<sup>[19]</sup> and corrected for absorption by a semi-empirical method (comparison of Laue equivalents), with the SADABS program.<sup>[20]</sup> The structures were solved by direct methods and refined by full-matrix least squares against  $F^2$  of all data by using SHELXTL software.<sup>[21]</sup>

**Crystal data:**  $\text{C}_{24}\text{H}_{20}\text{S}_8^{2+}(\text{ClO}_4^-)_2$ ,  $M_r = 763.78$ ,  $T = 103\ \text{K}$ , monoclinic, space group  $P2_1/c$  (No. 14),  $a = 16.206(1)$ ,  $b = 7.798(1)$ ,  $c = 12.819(1)\ \text{\AA}$ ,  $\beta = 112.09(1)^\circ$ ,  $U = 1501.1(2)\ \text{\AA}^3$ ,  $Z = 2$ ,  $\mu = 0.82\ \text{mm}^{-1}$ , 15578 reflections ( $2\theta = 55^\circ$ ) of which 3450 unique,  $R_{\text{int}} = 0.039$ , 196 refined parameters,  $R = 0.031$  [2888 data with  $F^2 = \sigma(F^2)$ ],  $wR(F^2) = 0.076$ . Crystallographic data (excluding structure factors) have been deposited with the Cambridge Crystallographic Data Centre as supplementary publication no. CCDC-148475. Copies of the data can be obtained free of charge on application to

CCDC, 12 Union Road, Cambridge CB2 1EZ, UK (Fax: (+44)1223-336033; E-mail: deposit@ccdc.cam.ac.uk).

### Acknowledgements

This work was funded by the EPSRC. We thank Dr. I. Clark for technical assistance with recording the Raman spectra and Prof. N. Martín for a preprint of ref. [12].

- [1] a) F. Wudl, G. M. Smith, E. Hufnagel, *J. Chem. Soc. Chem. Commun.* **1970**, 1453–1454; b) S. Hünig, G. Kiesslich, H. Quast, D. Scheutzow, *Liebigs Ann. Chem.* **1973**, 310–323; c) M. R. Bryce, *J. Mater. Chem.* **2000**, *10*, 589–598.
- [2] T. K. Hansen, J. Becher, *Adv. Mater.* **1993**, *5*, 288–292.
- [3] a) T. Sugimoto, H. Awaji, I. Sugimoto, Y. Misaki, T. Kawase, S. Yoneda, Z. Yoshida, *Chem. Mater.* **1989**, *1*, 535–547; b) M. R. Bryce, A. J. Moore, B. K. Tanner, R. Whitehead, W. Clegg, F. Gerson, A. Lamprecht, S. Pfenninger, *Chem. Mater.* **1996**, *8*, 1182–1188; c) A. J. Moore, M. R. Bryce, A. S. Batsanov, A. Green, J. A. K. Howard, M. A. McKerverve, P. McGuigan, I. Ledoux, E. Ortí, R. Viruela, P. M. Viruela, B. Tarbit, *J. Mater. Chem.* **1998**, *8*, 1173–1184; d) Y. Yamashita, M. Tomura, M. B. Zaman, M. Imaeda, *Chem. Commun.* **1998**, 1657–1658; e) J. Yamada, H. Nishikawa, K. Kikuchi, *J. Mater. Chem.* **1999**, *9*, 617–628.
- [4] a) Y. Yamashita, Y. Kobayashi, T. Miyashi, *Angew. Chem.* **1989**, *101*, 1090–1091; *Angew. Chem. Int. Ed. Engl.* **1989**, *28*, 1052–1053; b) A. J. Moore, M. R. Bryce, *J. Chem. Soc. Perkin Trans. 1* **1991**, 157–168.
- [5] For a review of multi-stage redox systems see: S. Hünig, H. Berneth, *Top. Curr. Chem.* **1980**, *92*, 1–44.
- [6] A. S. Batsanov, M. R. Bryce, M. A. Coffin, A. Green, R. E. Hester, J. A. K. Howard, I. K. Lednev, N. Martín, A. J. Moore, J. N. Moore, E. Ortí, L. Sánchez, M. Savíron, P. M. Viruela, R. Viruela, T.-Q. Ye, *Chem. Eur. J.* **1998**, *4*, 2580–2592.
- [7] a) M. R. Bryce, M. A. Coffin, M. B. Hursthouse, A. I. Karaulov, K. Müllen, H. Scheich, *Tetrahedron Lett.* **1991**, *32*, 6029–6033; b) M. R. Bryce, T. Finn, A. S. Batsanov, R. Katakly, J. A. K. Howard, S. B. Lyubchik, *Eur. J. Org. Chem.* **2000**, 1199–1205.
- [8] a) M. R. Bryce, T. Finn, A. J. Moore, A. S. Batsanov, J. A. K. Howard, *Eur. J. Org. Chem.* **2000**, 51–60; b) M. R. Bryce, A. S. Batsanov, T. Finn, T. K. Hansen, A. J. Moore, J. A. K. Howard, M. Kamenjicki, I. K. Lednev, S. A. Asher, *Eur. J. Org. Chem.* **2000**, in press. For recent reports of entirely different saddle-shaped molecules see: c) K. Yamamoto, H. Sonobe, H. Matsbara, M. Sato, S. Okamoto, K. Kitaura, *Angew. Chem.* **1996**, *108*, 69–70; *Angew. Chem. Int. Ed. Engl.* **1996**, *35*, 69–70; d) P. D. Croucher, J. M. E. Marshall, P. J. Nichols, C. L. Raston, *Chem. Commun.* **1999**, 193–194; e) J. Tellenbröker, D. Kuck, *Angew. Chem.* **1999**, *111*, 1000–1004; *Angew. Chem. Int. Ed.* **1999**, *38*, 919–921; f) H. Bock, Z. Havlas, K. Gharagozloo-Hubmann, M. Sievert, *Angew. Chem.* **1999**, *111*, 2379–2382; *Angew. Chem. Int. Ed.* **1999**, *38*, 2240–2243; g) I. Chambrier, M. J. Cook, P. T. Wood, *Chem. Commun.* **2000**, 2133–2134.
- [9] a) M. R. Bryce, A. J. Moore, M. Hasan, G. J. Ashwell, A. T. Fraser, W. Clegg, M. B. Hursthouse, A. I. Karaulov, *Angew. Chem.* **1990**, *102*, 1493–1495; *Angew. Chem. Int. Ed. Engl.* **1990**, *29*, 1450–1452; b) S. Triki, L. Ouahab, D. Lorcy, A. Robert, *Acta Crystallogr. Sect. C* **1993**, *49*, 1189–1192.
- [10] N. Martín, L. Sánchez, C. Seoane, E. Ortí, P. M. Viruela, R. Viruela, *J. Org. Chem.* **1998**, *63*, 1268–1279.
- [11] a) M. A. Herranz, N. Martín, L. Sánchez, J. Garín, J. Orduna, R. Alcalá, B. Villacampa, C. Sánchez, *Tetrahedron* **1998**, *54*, 11651–11658; b) M. A. Herranz, N. Martín, *Org. Lett.* **1999**, *1*, 2005–2007; c) C. A. Christensen, M. R. Bryce, A. S. Batsanov, J. A. K. Howard, J. O. Jeppesen, J. Becher, *Chem. Commun.* **1999**, 2433–2434; d) N. Martín, L. Sánchez, D. M. Guldi, *Chem. Commun.* **2000**, 113–114.
- [12] D. M. Guldi, L. Sánchez, N. Martín, personal communication.
- [13] A. Beeby, A. Jones, *Photochem. Photobiol.* **2000**, *72*, 10–15.
- [14] B. Scradler, *Raman: Infrared Atlas of Organic Compounds*, VCH, Weinheim, **1989**.
- [15] J. Casado, V. Hernández, Y. Kanemitsu, J. T. Lopéz Navarrete, *J. Raman Spec.* **2000**, *31*, 565–570.
- [16] C. P. Brock, J. D. Dunitz, *Acta Crystallogr. Sect. B* **1990**, *46*, 795–806.
- [17] Yu. V. Zefirov, P. M. Zorkii, *Russ. Chem. Rev.* **1995**, *64*, 415–428.
- [18] C. M. Duff, G. A. Heath, *Inorg. Chem.* **1991**, *30*, 2528–2535.
- [19] SMART & SAINT, *Area Detector Control and Integration Software, Version 6.01*, Bruker Analytical X-ray Systems, Madison, Wisconsin (USA), **1999**.
- [20] G. M. Sheldrick, *SADABS: Program for Scaling and Correction of Area Detector Data*, University of Göttingen (Germany), **1998**.
- [21] SHELXTL, *An Integrated System for Solving, Refining and Displaying Crystal Structures from Diffraction Data, Version 5.10*, Bruker Analytical X-ray Systems, Madison, Wisconsin (USA), **1997**.

Received: September 25, 2000 [F2748]